5

More Complex and Model Independent Pharmacokinetic Models

5.1 Introduction

In the previous chapter the fundamental principles of pharmacokinetics were discussed using the simplest of compartmental models. However, it is often the case that the plasma concentration–time data cannot be explained adequately using a single-compartment model, indeed it is difficult to find practical examples of drugs that conform to single-compartment pharmacokinetics after intravenous bolus doses. Generally, more complex, multi-compartment models are required, or it may not be possible to define a compartment model at all and other approaches are required. These are the topics of this chapter.

5.2 Multiple compartment models

5.2.1 Intravenous injections

Quite commonly, when the concentration data are plotted on logarithmic scales, the plot is curvilinear and may be described as the sum of two or more exponential decays. In this case a multiple-compartment model can be used [Figure 5.1(a)]. This is sometimes described as 'the drug conferring on the body the characteristics of a two-(or multi-) compartment model'.

The general equation for the plasma concentration, C, as a function of time in a multiple-compartment model, following an intravenous bolus injection is:

$$C = \sum_{i=1}^{n} C_i \exp(-\lambda_i t) \tag{5.1}$$

This is exemplified in Figure 5.2 which shows the blood concentrations of methylene blue after a bolus intravenous injection of 100 mg. Methylene blue is of some importance in medicine as a contrast agent and for evaluating body fluid volumes. However, it is also a life-saving drug used as an electron donor in the treatment of both congenital and drug-induced methaemoglobinaemia. It shows multiphasic decline of concentrations in plasma (Peter *et al*., 2000).

Drug Disposition and Pharmacokinetics: From Principles to Applications Stephen H. Curry and Robin Whelpton
 ISBN: 978-0-470-68446-7

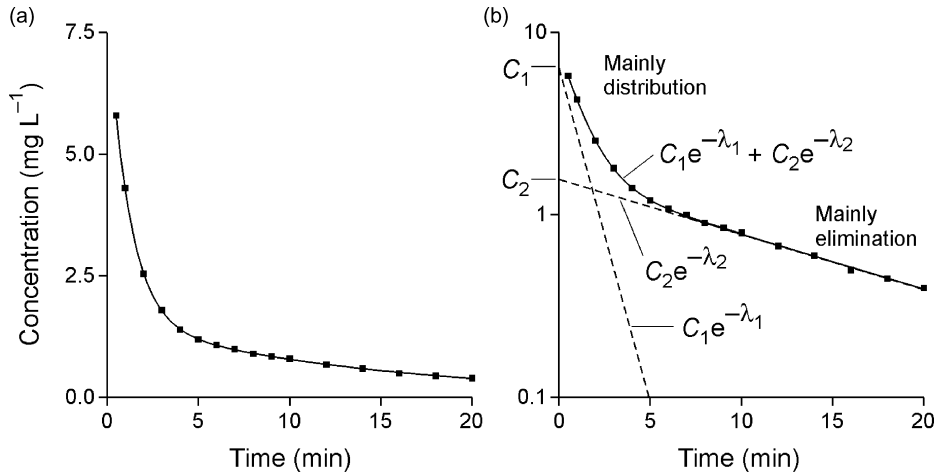

Figure 5.1 Example of data that fits a two-compartment model (a) Cartesian coordinates and (b) semi-logarithmic plot.

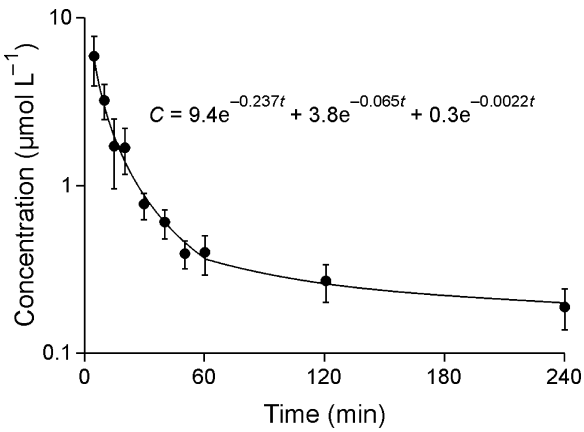

Figure 5.2 Blood concentrations of methylene blue (mean ± SEM, $n = 7$) after 100 mg intravenously. Data fitted using sum of three exponential terms (solid line). (Redrawn from Peter *et al.*, 2000).

For a two-compartment model, $n = 2$, and Equation 5.1 can be written:

$$C = C_1 \exp(-\lambda_1 t) + C_2 \exp(-\lambda_2 t) \tag{5.2}$$

Sometimes (particularly in American literature) Equation 5.2 is written as:

$$C = A \exp(-\alpha t) + B \exp(-\beta t) \tag{5.3}$$

Note that $\lambda_1 > \lambda_2$ ($\alpha > \beta$), as λ_1 (or α) is the rate constant of the steeper part of the decay curve. Indeed this initial steep part may be referred to as the 'α-phase'. The last exponential defines the *terminal* phase, and by convention the rate constant of this phase is λ_z. Thus, for a two-compartment model, $\lambda_2 = \beta = \lambda_z$. An example of a two-compartment model is depicted in Figure 5.3. Rather than the one homogeneous solution of drug of

the single-compartment, this model has two solutions, with reversible transfer of drug between them. By definition, plasma is always a component of the central compartment, sometimes called the plasma compartment. The other compartment is the peripheral or tissue compartment. The volumes of these compartments are V_1 and V_2 respectively. The use of other terms such as V_p, can lead to untold confusion – is

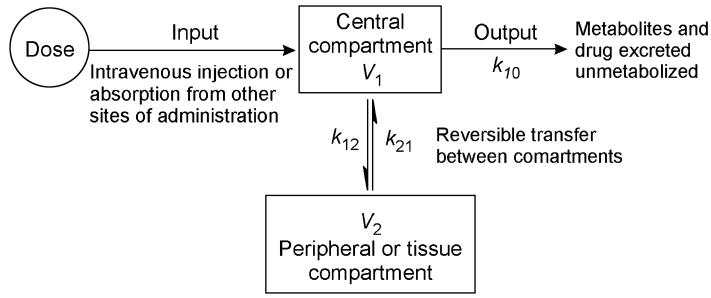

Figure 5.3 Diagrammatic representation of a two-compartment model.

that p for plasma or p for peripheral? The rate constants are labelled according to the direction of movement to which they refer, so the constant relating to transfer from the central (1) to the peripheral compartment (2) is k_{12}. The rate constant for loss from the central compartment by metabolism or excretion of unchanged drug is k_{10} (Figure 5.3) where 0 depicts compartment zero, that is outside the body. Other two-compartment models are possible where drug is metabolized or excreted from the peripheral compartment, or from both central and peripheral compartments. However, the liver and kidneys are often part of the central compartment so the model of Figure 5.3 is usually appropriate.

The shape of the curve of Figure 5.1(b) can be explained as follows:

- Shortly after injection there is rapid transfer of drug from plasma, in the central compartment, to the tissues of the peripheral compartment, with only a small proportion of the dose being eliminated during this time.
- At later times the concentration of drug in the compartments equilibrate and the decay from plasma is chiefly a result of elimination of drug from the body as a whole either by metabolism or excretion of unchanged drug.

5.2.1.1 Concentrations in the peripheral compartment

When the drug is injected at $t = 0$, instantaneous mixing in the central compartment is assumed. The initial concentration, $C_0 = C_1 + C_2$, and there is no drug in the peripheral compartment. Consequently, the concentration in the peripheral compartment increases until the forward and backward rates of transfer are equal and, for an instant, there is no net movement of drug. This condition is referred to as steady-state (not to be confused with the concept of steady-state discussed in the previous chapter in which the term was applied to equilibrium concentrations in plasma during long-term dosing), after which net transfer is from the peripheral to the central compartment, because elimination is reducing the concentration in the central compartment. Normally, the amount or concentration in the peripheral compartment is calculated using parameters derived from the plasma concentration–time data:

$$C_{\text{periph}} = \frac{D\,k_{12}}{V_2(\lambda_1 - \lambda_2)}[\exp(-\lambda_2 t) - \exp(-\lambda_1 t)] \tag{5.4}$$

Unlike the biological situation, it is possible to demonstrate this relationship, using the dyes as models as in the previous chapter. For example, methylene blue (see Figure 5.2) is a phenothiazine dye with an intense

blue colour – it was the dye mentioned in Chapter 4. Using the models described earlier, it was possible to generate the data in Figure 5.4 for distribution of methylene blue through a two-compartment model. This emphasizes the fact that the steady-state in question in this context is characterized by there being an instant in time when the concentrations in the two compartments are identical and there is no net movement of drug between the compartments.

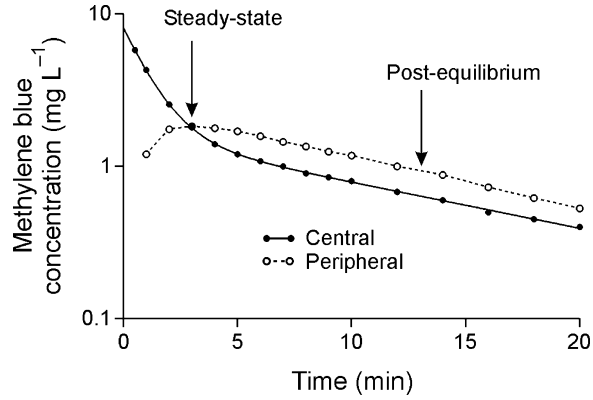

Figure 5.4 Simulation of a two-compartment compartment model showing methylene blue concentrations in the central and peripheral compartments.

The central and peripheral compartment curves cross when the concentration in the peripheral compartment is maximal. This must be the case because this is steady-state and the concentrations are equal. The time of the peak, t_{max} is:

$$t_{max} = \frac{1}{(\lambda_1 - \lambda_2)} \ln\left(\frac{\lambda_1}{\lambda_2}\right) \tag{5.5}$$

At later times (in theory, only at infinite time) the compartments equilibrate and the *ratio* of concentrations remains constant – shown as a parallel decline on a semilogarithmic plot (Figure 5.4).

5.2.1.2 Microconstants

The rate constants of Figure 5.3 are known as microconstants and have to be derived from C_1, C_2 λ_1 and λ_2, which are obtained by resolving the plasma concentration–data into its two exponential terms (Section 5.2). The sum of the microconstants equals the sum of λ_1 and λ_2:

$$\lambda_1 + \lambda_2 = k_{10} + k_{12} + k_{21} \tag{5.6}$$

and

$$k_{21} = \frac{C_1\lambda_2 + C_2\lambda_1}{C_1 + C_2} \tag{5.7}$$

$$k_{10} = \frac{\lambda_1\lambda_2}{k_{21}} \tag{5.8}$$

$$k_{12} = \lambda_1 + \lambda_2 - k_{10} - k_{21} \tag{5.9}$$

Confusion sometimes arises over the relationship between k_{10} and λ_2. The former is the rate constant for loss of drug from the central compartment and is greater than λ_2, which is the rate constant for loss of drug from the body and is derived from the terminal phase of the plasma concentration–time curve once equilibrium has been fully established. The value of λ_2 may be influenced by the other rate constants, particularly k_{21} which controls the rate of return of drug from tissues to the central compartment.

The importance of calculating the microconstants is that they are required to calculate the apparent volumes of distribution. Also, k_{10} and λ_2 are affected differently by diseases and in 'special populations' (Chapters 9, 11 and 12) and this can be very important in understanding requirements for dosing in such populations.

5.2.1.3 Apparent volumes of distribution

Adopting the same approach as that for the single-compartment model, the volume of the central compartment is:

$$V_1 = \frac{D}{C_0} = \frac{D}{C_1 + C_2} \tag{5.10}$$

because at $t = 0$ none of the dose has been transferred to the peripheral compartment, and C_0 is the sum of the constants of the two exponential terms. At steady-state, the concentrations in each compartment are equal, and the forward and backward rates are equal as there is (instantaneously) no net movement of drug:

$$V_1 C_{ss}\, k_{12} = V_2 C_{ss}\, k_{21} \tag{5.11}$$

Cancelling C^{ss} and rearranging gives:

$$V_2 = V_1 \frac{k_{12}}{k_{21}} \tag{5.12}$$

The apparent volume of distribution at steady-state, V_{ss} is the sum of apparent volumes of the individual compartments:

$$V_{ss} = V_1 + V_2 \tag{5.13}$$

The volume of distribution throughout the body at steady-state indicates the extent to which the drug is distributed throughout the body. In the methylene blue experiment it is in good agreement with the notional total volume (Table 5.1). However, it is clear from Figure 5.4 that the only time that multiplying V_{ss} by the plasma concentration will give the true amount of drug in the body is that instant at which steady-state conditions occur. Post-equilibrium, using V_{ss} will give an underestimate of the amount of drug in the body

Table 5.1 Results from i.v. injection of methylene blue into a two compartment model

Parameter	Found	Parameter	Found	Parameter	Found	Notional
Dose (mg)	4[a]	C_0 (mg mL^{-1})	8.13	V_1 (mL)	492	500
C_1 (mg mL^{-1})	6.56	k_{21} (min^{-1})	0.219	V_2 (mL)	965	1000
λ_1 (min^{-1})	0.847	k_{10} (min^{-1})	0.267	V_{ss} (mL)	1457	1500
C_2 (mg mL^{-1})	1.57	k_{21} (min^{-1})	0.430	V_{Area} (mL)	1902	n.a.[b]
λ_2 (min^{-1})	0.0691			CL (mL min^{-1})	131.5	130

[a]Not calculated.
[b]Not applicable.

because the peripheral concentrations are higher than those in plasma. Consequently a further calculation of apparent volume of distribution is required, V_{Area}:

$$V_{\text{Area}} = \frac{D}{AUC\,\lambda_2} \tag{5.14}$$

This apparent volume of distribution is best thought of as a constant of proportionally that allows the amount of drug in the body to be calculated post-equilibrium. Furthermore, V_{area} changes with changes in clearance (which changes λ_2). This must be the case because considering Figure 5.4, as clearance increases the plasma concentrations fall but the concentrations in the peripheral compartment do not fall to the same extent and so V_{area} is greater (Table 5.1). If there was no clearance the drug would not be removed from the body and the concentrations in the central and peripheral compartments would be equal, that is $V_{\text{area}} = V_{\text{ss}}$.

The term V_{extrap}, which uses a construction line through the terminal phase of the plasma concentration data extrapolated to $t = 0$ may be encountered, particularly in older literature. In the example of Figure 5.3, the intercept is C_2, and $V_{\text{extrap}} = D/C_2$, is analogous to the one-compartment case. This approach overestimates the apparent volume of distribution, particularly when V_2 is large relative to V_1. For example using the data of Table 5.1 D/C_2 calculates to be 2550 mL, larger than both V_{ss} and V_{area}.

5.2.1.4 Clearance

The area under the curve is the sum of the areas under the two exponential phases so, by analogy with Equation 4.11, for a two compartment model:

$$AUC = \frac{C_1}{\lambda_1} + \frac{C_2}{\lambda_2} \tag{5.15}$$

Several approaches may be used to calculate clearance. Equation 4.14 is applicable to single- and multiple-compartment models, and if *AUC* is obtained using the trapezoidal method it is not even necessary to define the number of compartments (Section 5.3):

$$CL = \frac{D}{AUC} \tag{4.14}$$

As the rate of elimination from the body $= C \times CL$, where C is the plasma concentration (or the concentration in V_1) then the rate of elimination from/via the central compartment/plasma is the amount $(V_1 \times C)$ multiplied by the elimination rate constant, k_{10}:

$$C \times CL = V_1 \times C \times k_{10} \tag{5.16}$$

Cancelling C from each side gives:

$$CL = V_1 k_{10} \tag{5.17}$$

Post-equilibrium, it has been shown (Gibaldi and Perrier, 1982) that:

$$V_{\text{area}}\,\lambda_2 = V_1 k_{10} \tag{5.18}$$

and substituting Equation 5.17 gives:

$$CL = V_{\text{area}}\,\lambda_2 \tag{5.19}$$

The amount of drug in the body post-equilibrium is V_{area} multiplied by the plasma concentration so the rate of elimination, p*ost-equilibrium* is: $(V_{\text{area}} \times C)\,\lambda_2$.

5.2.2 Absorption

The addition of an absorption phase to the arithmetic of a two-compartment model leads to an extremely complex situation. A working equation for first-order absorption into a two compartment model is:

$$C = C_1' \exp(-\lambda_1 t) + C_2' \exp(-\lambda_2 t) - (C_1' + C_2') \exp(-k_a t) \tag{5.20}$$

The values C_1' and C_2' are not the same as C_1 and C_2 as they are affected by both the rate and extent of absorption. The situation is further complicated by the relative sizes of the rate constants. If the rate constant of absorption is large then it may be possible to resolve the data and obtain estimates of k_a, λ_1 and λ_2 (Figure 5.4). However, it is often not possible to ascribe values to k_a and λ_1 without investigating the kinetics using an intravenous dose. Furthermore, when $k_a < k_{21}$ the distributional phase is not apparent and the model appears to be that of a single compartment (Figure 5.5). In this situation one could not define a two compartment model without also using an intravenous dose.

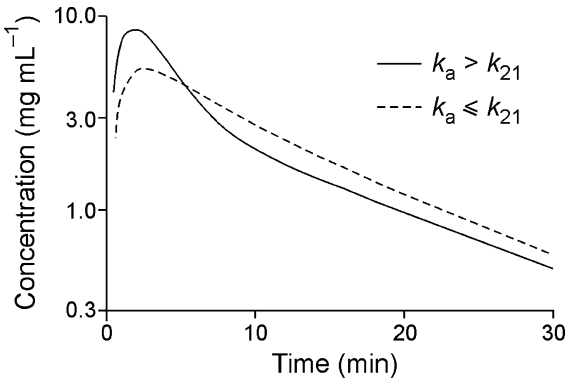

Figure 5.5 Absorption into a two-compartment model.

5.2.3 Infusions

When a drug is infused into a two-compartment model the shape of the rising phase is the inverse of the decay curve at the end of the infusion, just as it was in the single compartment case (Section 4.2.5). Thus the rising phase is composed of two exponential terms, with an initial steep rise. When the infusion is stopped it may be possible to resolve the decay curve into two exponential terms, depending on the relative sizes of C_1 and C_2. The initial steep phase is not as obvious as that after an intravenous bolus injection because during the infusion drug has been transferred to the peripheral compartment and the concentration gradient between the two compartments is not as great, particularly as the concentration approaches steady-state. When the infusion is stopped the exponential curves can be extrapolated to give intercepts, C_1' and C_2' on a vertical construction line drawn at the time the infusion was stopped. If the infusion were continued to steady-state the relationships to C_1 and C_2 are:

$$C_1 = \frac{D\, C_1' \lambda_1}{R_0} \tag{5.21}$$

and

$$C_2 = \frac{D\, C_2' \lambda_2}{R_0} \tag{5.22}$$

where D is the accumulated dose during the infusion (i.e. R_0T). As previously, R_0 is the zero-order infusion rate.

It is possible to calculate a loading dose, R_0/k_{10}, to give an instantaneous steady-state concentration, C^{ss}, in plasma. However, this ignores the transfer of drug from the central to the peripheral compartment and so initially the plasma concentration falls and then rises and asymptotes to C^{ss}. Again this can be demonstrated empirically using methylene blue [Figure 5.6(a)]. To avoid the plasma concentrations during the infusion falling below C^{ss}, a larger loading dose, R_0/λ_2, has to be used, but this may result in the initial concentrations being unacceptably high [Figure 5.6(b)]. This problem is of practical importance for some drugs, for example when lidocaine is used to control ventricular arrhythmias. One solution is to use a 'loading infusion', that is to infuse at a higher rate initially and then reduce the rate to that required for the desired steady-state concentration. An alternative scheme, using intravenous administration of an initial bolus loading dose in conjunction with a constant rate and an exponential intravenous drug infusion has been proposed (Vaughan and Tucker, 1976).

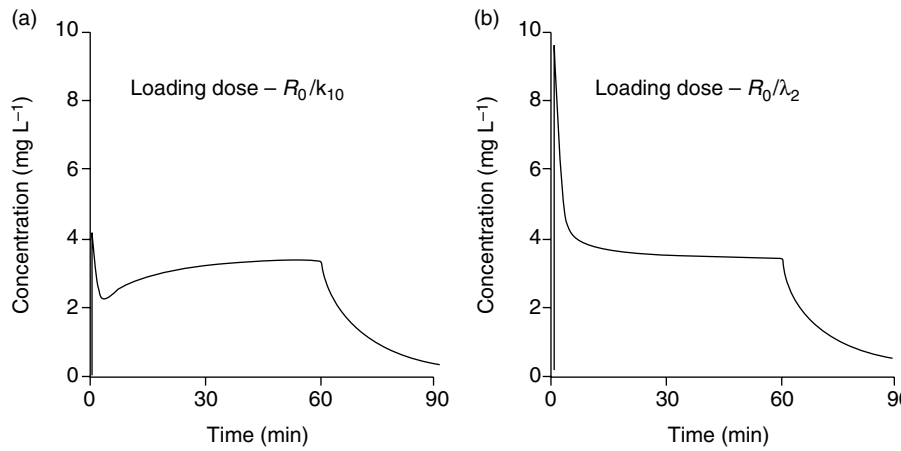

Figure 5.6 Infusion into a two-compartment model with different loading doses. (a) R_0/k_{10} gives instantaneous steady-state concentration, but this falls as drug is transferred to the peripheral compartment. (b) A loading dose R_0/λ_2 ensures the concentrations do not fall below C^{ss}, but the peak concentration may be unacceptably high.

5.2.4 Multiple oral dosing

The principles outlined in Chapter 4 apply. On repeated dosing the plasma concentrations will increase and tend towards steady-state conditions. As before the situation is simpler at steady-state when following repeated intravenous doses:

$$C = C_1' \exp(-\lambda_1 t) + C_2' \exp(-\lambda_2 t) \tag{5.23}$$

where t is any time during the dosage interval and

$$C_1' = C_1 \left(\frac{1}{1 - \exp(-\lambda_1 \tau)} \right) \tag{5.24}$$

and

$$C_2' = C_2\left(\frac{1}{1-\exp(-\lambda_2\tau)}\right) \tag{5.25}$$

and τ is the dosing interval. The average plasma concentration at steady-state is given by:

$$C_{\text{av}}^{\text{ss}} = \frac{AUC}{\tau} = \frac{FD}{V_1\, k_{10}\, \tau} = \frac{FD}{V_{\text{Area}}\lambda\tau} \tag{5.26}$$

See also Equation 4.38.

5.2.5 Concept of compartments

The concept of pharmacokinetic compartments may be difficult for anyone new to the topic. Understanding is not helped by the fact on some occasions the volume of a 'pharmacokinetic' compartment may be identical to a known anatomical volume such as plasma or total body water, but more often than not the calculated and anatomical volumes of distribution bear no comparison. Then there is the question of which tissues constitute a particular compartment. Generally, well-perfused tissues are components of the central compartment for lipophilic drugs as lipid membranes provide little in the way of a barrier to the movement of such drugs, and tissue and plasma concentrations rapidly equilibrate. Such tissues include liver and kidney and often brain (Figure 5.7). Thus, although the concentrations in individual tissues may be different, the kinetics describing the changes in concentrations are the same, and they decline in parallel on a semi-logarithmic plot (e.g. plasma and liver in Figure 2.13(a)). For a lipophilic drug, the rate of delivery (blood flow) to the tissue is important and so equilibration with the less well-perfused tissue is slower and apparent from the plasma concentration–time plot. In this situation, such tissues constitute the peripheral compartment and might include fat and muscle (Figure 5.7).

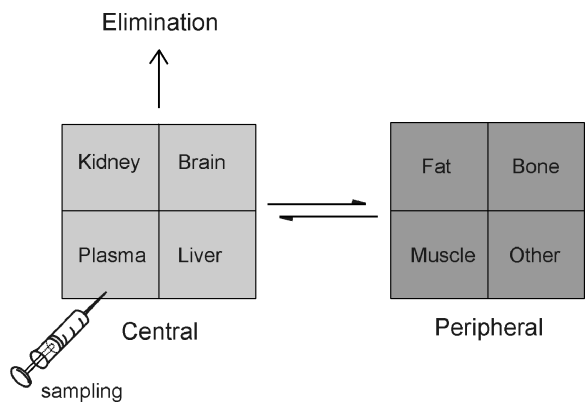

Figure 5.7 Representation of tissues that might constitute the central and peripheral compartments for a lipophilic drug.

It is worth remembering that (i) concentration–time plots, particularly with human subjects, are of plasma or blood, (ii) concentrations in tissues of the central compartment are usually higher than those in plasma and (iii) the concentrations in the peripheral compartment(s) will rise as drug is distributed from the central compartment.

5.2.6 Relationship between dose and duration of effect

The relatively simple relationship between dose and duration of effect for a single-compartment model was discussed in Section 4.4. The situation is more complex for multiple-compartment models but these are necessary to explain the duration of action of many drugs. This is best exemplified by thiopental, which clearly exhibits multiple-compartment kinetics (Figure 2.14). Liver concentrations rapidly equilibrate with those in plasma whilst the concentrations in skeletal muscle rise initially and then equilibrate. The concentrations in adipose tissue rise for at least the first 3.5 hours of the experiment. Therefore thiopental needs at least three compartments: a central and two peripheral compartments (Figure 5.8).

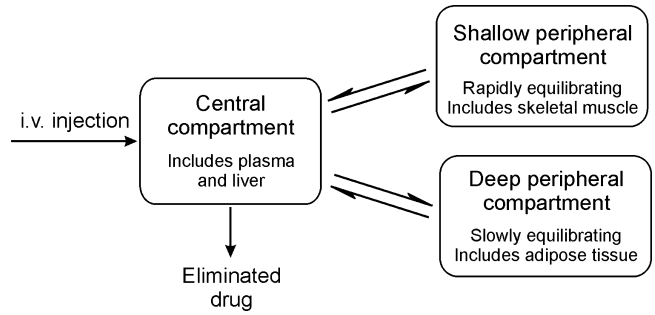

Figure 5.8 Thiopental kinetics require three compartments.

As discussed in Section 2.4.4.1, following an i.v. bolus injection of thiopental the duration of action is short due to uptake of the drug into skeletal muscle and fat. When the drug was originally introduced and larger doses were injected or, more particularly, when doses were repeated, the duration of action was found to be disproportionately long. When dosing was carried out cautiously, noting the patient's response, and using a flexible dosing policy, long-term anaesthesia could be safely maintained. However, incautious administration, generally with a fixed-dose regimen unrelated to patient response led to each successive dose exerting a duration of action longer than the previous one, until an excessively long duration of action occurred, even when administration ceased. It has been incorrectly assumed that this phenomenon is due to saturation of tissue stores leading to increasing proportions of subsequent doses being unable to redistribute from plasma and brain. In fact there is no evidence of tissue saturation (Table 5.2) and the observation can be explained in terms of a multiple-compartment model.

Table 5.2 Duration of action and tissue localization of thiopental at four doses in man (adapted from Curry, 1980)

Dose (g)	Administration time (min)	Duration (h)	Amount in blood at 1 h (g)	Amount in tissues at 1 h (g)	T/B^a
0.4	2	0.25	0.027	0.333	12.3
1	5	0.5–1	0.066	0.834	12.6
2	5	1.5–2.5	0.156	1.744	11.1
3.8	50	4–6	0.288	3.512	12.2

[a]Tissue to blood ratio.

Using composite data for plasma concentrations in human subjects from Brodie's work and *assuming* a two-compartment model (the original work could be fitted to a three-compartment model in agreement with the results for dogs) plasma concentration decay curves for 0.5 and 0.75 g doses were calculated

(Figure 5.9). The subject from whom the data of Figure 5.9 were derived, was anaesthetized with a dose of 0.5 g (i.v.) and regained consciousness after 20 minutes when the plasma concentration was 6.99 mg L^{-1}. The kinetic model predicts that the subject would be unconscious for 2.8 h had the dose been increased by only 1.5-fold to 0.75 g. This is clearly a different situation from that predicted for intravenous injection into a single-compartment model (Section 4.4).

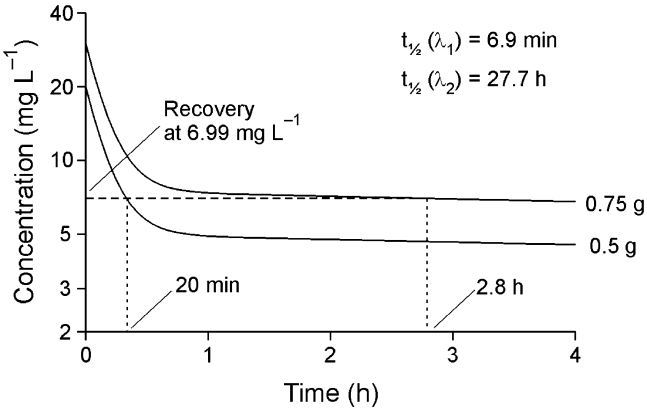

Figure 5.9 Time course of thiopental in plasma calculated from the composite data of Brodie following idealized doses of 0.5 and 0.75 g.

Additionally, the mean terminal half-life of thiopental has been shown to be different in lean and obese subjects, being 6.33 and 27.9 h, respectively, the variations being due to differences in apparent volumes of distribution rather than clearance (Jung *et al.*, 1982). Thus, the curve of Figure 5.9 may represent a more extreme situation than the average, but it does illustrate a general phenomenon applicable to all multiple-compartment models. It is apparent from the figure that the relative duration of effects will vary depending on the concentration at which recovery occurs. If recovery occurred post-equilibrium, during the terminal phase, then the relationship would be the same as that for the single-compartment model. Similarly, if recovery where largely during the distribution phase the increment in duration would not be so great, until of course the dose was increased to the point that recovery occurred in the terminal phase.

The effect of repeating the dose at the time of recovery, and at the same interval subsequently, can be modelled using:

$$C_n = C_1\left(\frac{1-\exp(-n\lambda_1\tau)}{1-\exp(-\lambda_1\tau)}\right)\exp(-\lambda_1 t) + C_2\left(\frac{1-\exp(-n\lambda_2\tau)}{1-\exp(-\lambda_2\tau)}\right)\exp(-\lambda_2 t) \qquad (5.27)$$

Where C_n is the concentration at time t following the n^{th} dose, C_1 and C_2 are the y-intercepts, following the intravenous bolus injection, and τ is the dosage interval (20 min in this example). This is illustrated in Figure 5.10.

While it is the case that with subsequent doses the rate of transfer from the central to the peripheral compartment will decline as the concentration in the peripheral compartment increases, this should not be confused with *saturation* of tissues. Saturation would lead to a change in the rate constants. Furthermore, the clinical situation will be even more complex because of the potential influence of tolerance, both receptor and pharmacokinetic, and the presence of other drugs.

The thiopental research described above was of seminal significance in the pursuit of pharmacokinetic understanding during the development of intravenous anaesthesia and analgesia, and thiopental continues to

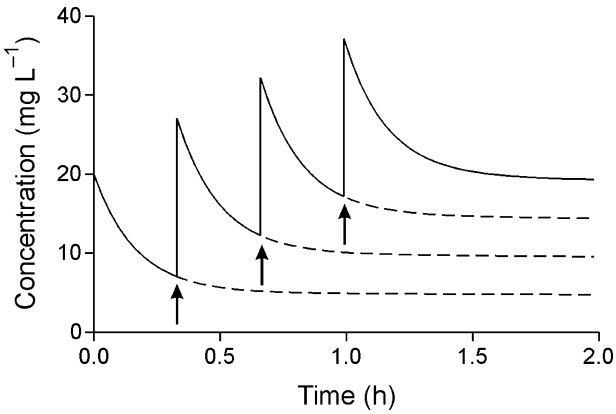

Figure 5.10 Modelled curves showing the effect of repeat injections (arrows) of thiopental at 20 minute intervals using the parameters of Figure 5.9.

be an anaesthetic of significance. Similar pharmacokinetic events are involved in the use of diazepam in status epilepticus, and in delirium tremens of alcohol withdrawal, with the added need in this case to avoid administration that is so rapid that the diazepam comes out of solution in the bloodstream before the injection solution is adequately diluted in the body. However, the most obvious modern example of a drug that follows the properties of the thiopental model is propofol, which is used as an intravenous sedative and anaesthetic, with or without other anaesthetics concurrently, particularly in out-patient procedures such as colonoscopies. Propofol concentrations rise rapidly during the early stages of infusion, then more slowly, even with constant rate infusion (as would be expected for a drug imparting the characteristics of a multiple-compartment model). The drug equilibrates very rapidly with the brain, so the effect is induced quickly, after which it is usually desirable to reduce the rate of infusion to maintain the effect while avoiding the excessive anaesthesia that could develop, relatively slowly, with prolonged administration. A distribution model analogous to that in Figure 5.8 has been devised for this drug. If drug infusion is discontinued after approximately 1 to 24 hours, the concentrations in the plasma decline rapidly and recovery is fast. If administration is for longer, for example for as long as 1 week, in the intensive care unit, the effect declines slowly on cessation of dosing as the terminal half-life is approximately 2 days (Knibbe *et al.*, 2000; Tozer and Rowland, 2006).

5.3 Curve fitting and choice of most appropriate model

Previously, reference has been made to resolving or fitting concentration–time data to obtain estimates of the pharmacokinetic parameters. However, discussion has been left until now because it easier to understand the underlying principles by considering resolution of the decay curve of a two-compartment model into its component exponential terms.

5.3.1 Graphical solution: method of residuals

Before the ready availability of personal computers and relatively inexpensive curve-fitting software, pharmacokinetic parameters were often obtained graphically. Although rarely used these days, an understanding of the approach is important when assessing the quality of the data to be analysed. The method of residuals, as it is known, is most easily understood from consideration of an intravenous bolus injection into a

two-compartment model. The data are plotted as a semi-logarithmic graph [Figure 5.1(b)]. Because $-\lambda_1$ is the slope of the steeper, initial phase, $\lambda_1 > \lambda_2$ and so the term $C_1\exp(-\lambda_1 t)$ approaches zero faster than $C_2\exp(-\lambda_2 t)$. Therefore at later times the contribution from the first exponential term is negligible and Equation 5.2 approximates to:

$$C \cong C_2 \exp(-\lambda_2 t) \tag{5.28}$$

Provided the plasma concentration–time curve is monitored for long enough, the terminal portion of the $\ln C$ versus t curve, will be a straight line so C_2 and λ_2 can be estimated [Figure 5.1(b)], from the y-intercept and slope of the terminal phase. Values of $C_2\exp(-\lambda_2 t)$ are calculated for earlier time points [i.e. when $C_1\exp(-\lambda_1 t)$ is making a significant contribution to the plasma concentration] and subtracted from the experimental values at those times to give estimates of $C_1\exp(-\lambda_1 t)$, which are referred to as *residuals*. A semilogarithmic plot of the residuals should give a straight line of slope $-\lambda_1$ and intercept C_1. Concave curvature of the residual line indicates that the first estimate of λ_2 is too low, whilst convex curvature indicates that it is too high, assuming that the data fit a two-compartment model.

The method of residuals can be applied to the majority of compartment models, and also first-order input into single- or multiple-compartments, and the post-infusion phase of zero-order infusions. Clearly, the method could not be used for situations where $k_a = \lambda$ as there is no linear phase to which a construction line can be drawn [Figure 4.8(b)]. These data can be fitted iteratively as described below.

5.3.2 Iterative curve-fitting

There are several commercially available curve-fitting programs that are sold specifically for pharmacokinetic analyses. However, other packages may be adapted to derive pharmacokinetic parameters. Concentration–time data for an intravenous bolus injection into a single compartment can be transformed to $\ln C$ versus t and solved using linear regression programs available on many hand-held calculators (but see Section 5.2.2.1). Many relationships do not have a mathematical solution and have to be solved iteratively, usually by computing the equation which gives the lowest residual sum of squares. On this occasion 'residual' refers to the difference between the observed value and the value calculated from the derived parameters. The square of the residuals is used because the residuals will be positive or negative. A useful source code for iterative curve fitting is that written in BASIC by Neilsen-Kudsk (1983). This code can be modified to run under different forms of BASIC and it is relatively easy to modify so that it can used to fit a wide variety of equations including calibration curves, most compartmental pharmacokinetic relationships and pH-extraction curves (Whelpton, 1989). With this robust algorithm several sets of data can be fitted to common parameters, for example concentration-time data following oral and i.v. administration of a drug, or after modification, complex (biphasic) dose-response curves in the presence of several concentrations of a competitive antagonist (Patel *et al*., 1995).

5.3.2.1 Weighted-regression

Experimental data will have associated errors. Linear regression assumes that the errors are the same irrespective of the concentration, that is, the data are homoscedastic. However, the size of the error generally increases with concentration – indeed most assays are developed to ensure that the relative standard deviations (RSD) cover a limited range and never exceed a predefined limit, say 10%. Therefore the errors are approximately proportional to the concentration and so the errors associated with high concentrations are higher and may unduly affect the way in which the data are fitted. Because unweighted regression treats all points equally, the fit will be biased towards the higher concentrations at the expense of the lower concentrations. This is particularly a problem with pharmacokinetic data as the concentrations often

extend over several orders of magnitude. The answer is to weight the data and to minimize the sum of weighted squares:

$$\text{weighted sum of residual squares} = \sum[(\text{weight})(\text{residual})^2] \tag{5.29}$$

The size of the random errors is assessed by the variance (s^2) and, ideally, the data should be weighted by $1/s^2$, so Equation 5.29 can be written:

$$\text{weighted sum of residual squares} = \sum[1/s^2(\text{residual})^2] \tag{5.30}$$

Thus, the points with the lowest errors assume more importance than those with the largest errors. Ideally, the points should be weighted by 1/variance, but it is unlikely that this will have been measured at every concentration because that would require replicate assays of every sample. However, if the RSD is (approximately) constant over the concentration range, then s is proportional to concentration and the data can be weighted $1/(\text{concentration})^2$. Many commercially-available statistical programs allow the option of weighting data by $1/y^2$.

Weighting data is not some method of manipulating the result to make it appear more acceptable, *it is the correct statistical treatment for heteroscedastic data*. However, this being said, when the errors are small and the concentration range limited, then there may be little difference in the values obtained by using non-weighted or weighted data. It should be noted that if ln C values are fitted, the transformation weights the data and the results are likely to be different from those when C versus t is fitted.

5.3.2.2 Choice of model

The number of compartments required to fit the data is given by the number of exponential terms that describe the *declining* portion of the curve. The choice of how many compartments to fit should be dictated by the data. Statistical fitting allows the various equations to be compared. Simply choosing the equation which gives the lowest residual sum of squares (SS) is unhelpful because this will be the equation with the largest number of parameters. Consequently, most statistical packages compute 'goodness of fit' parameters which take into account the number of parameters in the equation. Some programs will fit two equations simultaneously and compare them using the F-test. Neilsen-Kudsk (1983) used the Akaike information criterion (AIC):

$$AIC = N\ln(SS) + 2M \tag{5.31}$$

where N is the number of data points and M is the number of parameters. The equation with the lowest AIC is statistically the most appropriate.

The appropriateness of the model, including the weighting, should be tested by plotting the residuals as a function of concentration. These should be randomly distributed about zero. The correlation coefficient, r, is often a poor indicator of the goodness of fit – unless $r^2 = 1$!

5.3.3 Quality of the data

Whether the parameters are derived using the method of residuals or iterative computer fitting the results will be poor if the original data are poor. With modern analytical methods one would expect the concentration data to be reasonably accurate. The chief reasons for poor results are:

- Insufficient number of data points
- Incorrect timing of collection
- Data not collected for sufficient time.

The three bullet points above are related. If the model requires a large number of parameters, for example absorption into a three compartment model will generate seven parameters, then, clearly, the number of

points must be sufficient to ensure statistical significance – an absolute minimum of 8 (7 + 1). However, these points must be spaced at appropriate intervals so that each phase is defined, which is very unlikely to be the case with only eight samples. Another issue with timing is that the study design will usually specify the collection times, and these may be printed on the sample tubes prior to collection. It is not always possible to adhere to these times, which need not be a problem provided the correct time is recorded and used in the calculation. Use of uncorrected times will be more significant when the half-life is short. If the duration of the study is too short then the estimate of terminal rate constant, λ_z, is likely to be in error and this will be reflected in the estimates of the other parameters. The 'rule of thumb' is to collect data for at least $4 \times \lambda_z$. If a semi-logarithmic plot of the data does not show a more or less linear terminal phase then the results can be expected to be poor and using iterative fitting rather than the method of residuals will not improve them. It is a case of 'rubbish in = rubbish out'. For this reason data should always be plotted and inspected. In a study of temoporfin kinetics, the terminal half-life in blood was 13.9 h, when samples collected for up to 48 h were analysed; beyond which time the concentrations were too low to be quantified (Whelpton *et al*., 1995). However, the decay in brain and lung was much slower suggesting that 13.9 h was far too low an estimate. A second study using ^{14}C-labelled temoporfin showed that the terminal half-life in blood was ~10 days (Whelpton *et al*., 1996), a value that was confirmed from faecal excretion data collected for up to 5 weeks (Section 6.4). Some indication of for how long data should be collected can be obtained by modelling theoretical curves, as has been done for absorption into a two-compartment model (Curry, 1980).

5.4 Model independent approaches

5.4.1 Calculation of V_{Area} and clearance

Some of the pharmacokinetic parameters described above can be obtained without defining a model. Clearly, this applies to systemic availability, *F*, which is obtained by comparison of areas under the curve (Section 8.3). The *AUC*, calculated by the trapezoidal method, can used to derive systemic clearance and V_{Area} using Equations 4.26 and 5.14 or:

$$CL = F\frac{D}{AUC} \tag{4.26}$$

and

$$V_{\text{Area}} = F\frac{D}{AUC\,\lambda_z} \tag{5.14}$$

for extravascular doses. The data have to be such that the rate constant of the terminal phase can be derived. The approach can be illustrated using the data of Figure 5.5. Although it is not possible to define the correct number of compartments in one of the cases, the agreement between the parameters is good (Table 5.3). In

Table 5.3 Absorption of methylene blue into a two-compartment model with different rate constants of absorption

Parameter	Rapid absorption	Slow absorption
Terminal rate constant, λ_z (min^{-1})[a]	0.0679	0.0719
$AUC_{(0\text{-}30)}$ (mg min L^{-1})	68.5	67.9
C_{30}/λ_z (mg min L^{-1})	7.2	8.0
$AUC_{(0\text{-}\infty)}$ (mg min L^{-1})	75.7	75.9
CL/F (mL min^{-1})	132.1	131.8
V_{Area}/F (mL)	1946	1833

[a]From last five data points.

this particular instance we know that $F = 1$ and the clearance value is very close to the nominal flow rate of $130\,\text{mL}\,\text{min}^{-1}$.

Also, the average steady-state concentration can be obtained without defining number of compartments, Equation 5.26.

5.4.2 Statistical moment theory

Although statistical moment theory (SMT) is sometimes described as being non-compartmental, it does assume that the drug is measurable in plasma and also that the rate of elimination (flux) of drug is proportional to the plasma concentration (i.e. linear kinetics apply). The parameters that can be assessed are limited, but they are derived from measurements of areas under the curve without having to define compartments and assign, what can be ambiguous, rate constants to them. The method is useful when designing dosage regimens and interspecies extrapolations.

If one considers how long a single drug molecule stays in the plasma after administration, then it could be very short, very long or some intermediate interval, which is not particularly useful in itself. However, if large numbers of molecules are considered then there will be a mean residence time, *MRT*, which according to statistical moment theory is:

$$MRT = \frac{\int_0^\infty Ct\,\mathrm{d}t}{\int_0^\infty C\,\mathrm{d}t} = \frac{AUMC}{AUC} \tag{5.32}$$

where *AUMC* is known as the area under the (first) moment curve. The relationship between these areas is depicted in Figure 5.11.

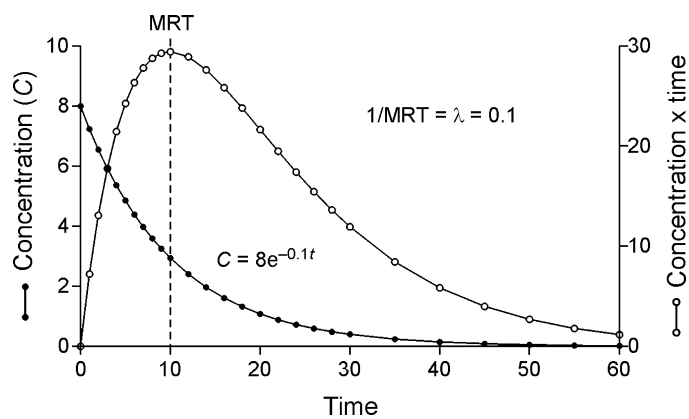

Figure 5.11 Model data for i.v. injection into a single-compartment, showing C versus t and Ct versus t.

For a bolus i.v. injection into a single-compartment model:

$$MRT_{\text{i.v}} = \frac{1}{\lambda} = \frac{V}{CL} \tag{5.33}$$

where λ is the rate constant of elimination. If comparing the results with a two-compartment model, then $MRT_{\text{i.v.}} = V_{\text{ss}}/CL$, and the apparent first-order rate constant has a value between λ_1 and λ_2. It follows from Equation 5.33 that *MRT* is the time when 63.2% of the intravenous dose will have been eliminated. This can be shown by substituting Equation 5.33 into Equation 1.8 when $t = MRT = 1/\lambda$:

$$C = C_0 \exp[-\lambda(1/\lambda)] = C_0 \exp(-1) = 0.368\, C_0 \tag{5.34}$$

Note that $\exp(-1) = 0.368$. As 36.8% remains, 63.2% must have been eliminated. The apparent volume of distribution at steady-state, V_{ss}, can be computed from:

$$V_{ss} = D\frac{AUMC}{AUC^2} = CL \times MRT \tag{5.35}$$

For first-order absorption, for example after an oral dose, the mean arrival time, *MAT*, can be used:

$$MAT = MRT_{\text{p.o.}} - MRT_{\text{i.v.}} \tag{5.36}$$

and

$$k_{\text{a}} = \frac{1}{MAT} \tag{5.37}$$

5.4.2.1 Estimating AUMC

The most obvious way of obtaining *AUMC* is to use the trapezoidal method, analogous to that used for *AUC* (see Appendix). The area of the n^{th} trapezium, $AUMC_n$, is:

$$AUMC_n = \frac{C_n + C_{n+1}}{2}(t_{n+1} - t_n)t_{n+1} \tag{5.38}$$

However, unlike *AUC*, the results are weighted by time, and the weight increases as the time increases. Also, Equation 5.38 overestimates the area, while using t_n underestimates *AUMC*. This can be reduced by using the midpoint for time:

$$AUMC_n = \frac{C_n + C_{n+1}}{2}(t_{n+1} - t_n)\frac{(t_n + t_{n+1})}{2} \tag{5.39}$$

Even so, Equation 5.39 overestimates the area for the decay part of the curve. A more accurate equation is:

$$AUMC_n = \frac{C_n(t_{n+1}^2 - t_n^2)}{2} + \frac{C_{n+1} - C_n}{6}(2t_{n+1}^2 - t_n t_{n+1} - t_n^2) \tag{5.40}$$

and, despite its complexity, is easy to use once it has been entered into an Excel spreadsheet. The area beyond the last time point is obtained by extrapolation:

$$AUMC_{(z-\infty)} = \frac{t_z C_z}{\lambda_z} + \frac{C_z}{\lambda_z^2} \tag{5.41}$$

where z denotes the last measured variable. Thus, despite being considered as a non-compartmental approach, it is necessary to calculate the terminal rate constant, which of course means identifying the last exponential phase.

5.4.2.2 Example of application of SMT

The data of Figure 5.1 were subjected to SMT (Figure 5.12). The first thing to note is that data have to be collected for a considerable time to define *AUMC* compared with that required to define two compartments from the *C* versus *t* data, as otherwise a large proportion of *AUMC* will be extrapolated. Obviously this has implications regarding the quality of the data because, in all probability, the errors will be highest at low concentrations and *AUMC* is weighted by the high values of *t*. Furthermore, the extrapolation of the remaining area requires accurate assessment of λ_z. Despite this, the results for the data of Figure 5.12 are in good agreement with those derived previously, reflecting the high quality of data (Table 5.4) in this case.

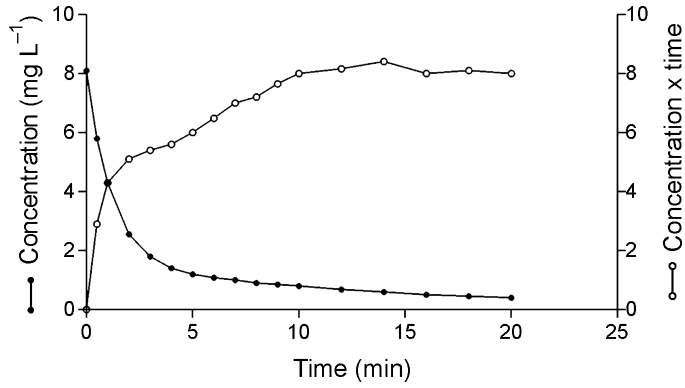

Figure 5.12 Statistical moment approach applied to the methylene blue data of Figure 5.1.

AUMC can be calculated for a compartmental model:

$$AUMC = \sum C_i/\lambda_i^2 \tag{5.42}$$

where *i* is the number of compartments. In the example of Table 5.4, Equation 5.42 gives $AUMC = 338.0\,\text{mg min}^2\,\text{L}^{-1}$.

Table 5.4 SMT approach to calculating pharmacokinetic parameters

Areas			Derived parameters	
Range (min)	*AUMC* (mg min^2 L^{-1})	*AUC* (mg min L^{-1})		
0–20	141.4[a]	25.0	*MRT* (min)	11.08
20–∞	199.5[b]	5.8	*CL* (mL min^{-1})[c]	130
0–∞	340.9	30.8	V_{ss} (mL)	1440

[a]Using Equation 5.40.
[b]From Equation 5.41.
[c]From Equation 5.35.

Thus the MRT is very easy to calculate, using only the *AUC* and the *AUMC* for a wide variety of pharmacokinetic systems. For one-compartment systems it provides a method for calculating the time for

63.2% of the dose to leave those systems, while for more complex systems it provides a straightforward means of evaluating changes caused by such factors as disease, age, interacting drugs, and many more, on the properties of the drug in question.

5.5 Population pharmacokinetics

This is an analytical process designed to focus on variability and central tendencies in data, and to optimize the use of 'sparse data', which is the type of data most often obtainable during Phase III studies, or after marketing of drugs. Typically, one or two blood samples are occasionally available from any one patient at this stage in the life cycle of a new drug. However, sparse data may be available from large numbers of patients. Thus, in Phase I trials, the investigations yield full pharmacokinetic profiles of investigational drugs in small numbers of healthy volunteers, often only male, and fitting a relatively narrow anthropomorphic profile. Phase II studies may extend this intensity of investigation to the target patient population, thus broadening the scope of the studies in regard to disease factors, interacting drugs, and such factors as age, but still with relatively small numbers of subjects. Later, the scope broadens, the numbers of patients becomes large, but the limitations of sparse data become especially important.

Population pharmacokinetics employs statistical methods based, in part, on a Bayesian feedback algorithm. These methods utilize the gradually accumulating pool of data to draw conclusions about physiological, disease, drug interaction, and other influences on the pharmacokinetic properties of the drug in the human population (Racine-Poon and Smith, 1990). Probability theory is used to facilitate step-by-step prediction of pharmacokinetic properties with ever greater precision, making possible better decisions on the choice of dose for various subpopulations, and eventually for individual patients, in the clinic. Because of this focus on the individual, some authors consider the label 'population statistics' to be unfortunate.

The methods of population statistics were pioneered by Sheiner and Beal (1982) and Whiting *et al*. (1986). Various statistical packages, in particular, and originally, NONMEM (Beal and Sheiner, 1982) have become synonymous with this work, although many others have found application (Aarons, 1991).

A different type of sparse data is obtained when just one sample can be obtained from each patient in a short-term time-dependent study of the type shown in Figure 5.13. This shows the anterior chamber (of the

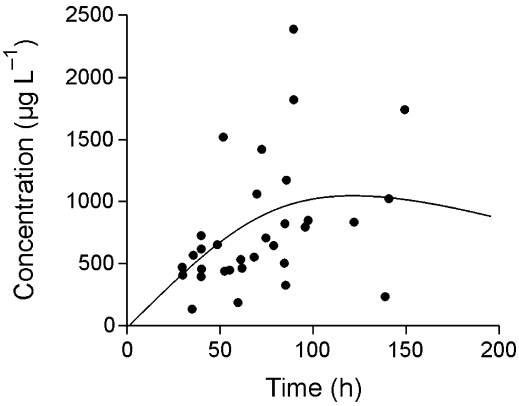

Figure 5.13 Distance-weighted least squares plot of correlation of time after application of ofloxacin and aqueous humour concentration. (Redrawn from Bouchard *et al.,* 1996).

eye – aqueous humour) ofloxacin concentrations in 32 patients each given the same drug regimen, a series of eye drops, at the time of cataract surgery. A statistically significant correlation between time since last dose and concentration was found ($r = 0.39; p = 0.025$) using least squares regression analysis, indicating that t_{max} occurred at $\sim$2 h. and that C_{max} was $\sim 1000\,\mu g\,L^{-1}$. While this was at best a crude experiment, and the correlation coefficient indicated that time since dose accounted for less than 16% of the concentration variance, it does provide useful guidance in timing of ofloxacin dosing in future patients of this type.

Experiments of this type have also been useful in laboratory animals, particularly toxicokinetic studies, when often only one blood sample can be obtained from each animal. Such experiments are sometimes described as providing 'descriptive pharmacokinetic data,' as they rarely involve any pharmacokinetic data analysis. While this is acceptable terminology, it is probably unwise to designate studies of this type as population pharmacokinetics.

5.6 Summary

This chapter has illustrated the need for more complex models to explain the kinetics and effects of drugs that cannot be explained using the simpler one-compartment model, and approaches that can be adopted when a model cannot be defined. More complex PK/PD relationships are considered in Chapter 14. The use of other samples (urine and faeces) and metabolites to study pharmacokinetics are considered in the next chapter.

References and further reading

Aarons L. Population pharmacokinetics: theory and practice. *Br J Clin Pharmacol* 1991; 32: 669–70.

Beal SL, Sheiner LB. Estimating population kinetics. *Crit Rev Biomed Eng* 1982; 8: 195–222.

Bouchard CS, King KK, Holmes JM. The kinetics of anterior chamber ofloxacin penetration. *Cornea* 1996; 15: 72–5.

Curry SH. *Drug Disposition and Pharmacokinetics*, 3rd edn. Oxford: Blackwell Scientific, 1980.

Gibaldi M, Perrier D. *Pharmacokinetics*, 2nd edn. New York: Marcel Dekker, 1982.

Haggard HW, Greenberg LA. Studies in the absorption, distribution, and elimination of ethyl alcohol II. The excretion of alcohol in urine and expired air, and the distribution of alcohol between air and water, blood and urine. *J Pharmacol Exp Ther* 1934; 52: 150–166.

Jung D, Mayersohn M, Perrier D, Calkins J, Saunders R. Thiopental disposition in lean and obese patients undergoing surgery. *Anesthesiology* 1982; 56: 269–74.

Knibbe CA, Aarts LP, Kuks PF, Voortman HJ, Lie AHL, Bras LJ, Danhof M. Pharmacokinetics and pharmacodynamics of propofol 6% SAZN versus propofol 1% SAZN and Diprivan-10 for short-term sedation following coronary artery bypass surgery. *Eur J Clin Pharmacol* 2000; 56: 89–95.

Neilsen-Kudsk F. A microcomputer program in BASIC for interative, non-linear data-fitting to pharmacokinetic functions. *Int J Biomed Computing* 1983; 14: 95–107.

Patel J, Trout SJ, Palij P, Whelpton R, Kruk ZL. Biphasic inhibition of stimulated endogenous dopamine release by 7-OH-DPAT in slices of rat nucleus accumbens. *Br J Pharmacol* 1995; 115: 421–6.

Peter C, Hongwan D, Kupfer A, Lauterburg BH. Pharmacokinetics and organ distribution of intravenous and oral methylene blue. *Eur J Clin Pharmacol* 2000; 56: 247–50.

Racine-Poon A, Smith AFM. Population models. In: Berry DA,editor. *Statistical Methodology in the Pharmaceutical Sciences*. New York: Marcel Dekker, 1990: 139–62.

Riviere JE. *Comparative Pharmacokinetics: Principles, Techniques, and Applications*. Chichester: John Wiley & Sons, 2003.

Sheiner LB, Beal SL. Bayesian individualization of pharmacokinetics: simple implementation and comparison with non-Bayesian methods. *J Pharm Sci* 1982; 71: 1344–8.

Tozer TN, Rowland M. *Introduction to Pharmacokinetics and Pharmacodynamics*. Philadelphia: Williams & Wilkins, 2006.

Vaughan DP, Tucker GT. General derivation of the ideal intravenous drug input required to achieve and maintain a constant plasma drug concentration. Theoretical application to lignocaine therapy. *Eur J Clin Pharmacol* 1976; 10: 433–40.

Whelpton R. Iterative least squares fitting of pH-partition data. *Trends Pharmacol Sci* 1989; 10: 182–3.

Whelpton R, Michael-Titus AT, Basra SS, Grahn M. Distribution of temoporfin, a new photosensitizer for the photodynamic therapy of cancer, in a murine tumor model. *Photochem Photobiol* 1995; 61: 397–401.

Whelpton R, Michael-Titus AT, Jamdar RP, Abdillahi K, Grahn MF. Distribution and excretion of radiolabeled temoporfin in a murine tumor model. *Photochem Photobiol* 1996; 63: 885–91.

Whiting B, Kelman AW, Grevel J. Population pharmacokinetics. Theory and clinical application. *Clin Pharmacokinet* 1986; 11: 387–401.

6

Kinetics of Metabolism and Excretion

6.1 Introduction

There are situations where it is necessary to define the kinetics of the metabolites of the drug under investigation. Intellectual curiosity apart, this is obviously the case for prodrugs for which the pharmacological properties reside in the metabolite. In some situations the drug and one or more its metabolites may be active, although not necessarily in the same way. Indeed the metabolite may be responsible for toxicity. The FDA has taken an interest in potentially toxic metabolites, particularly those unique to human beings, and issued its guidelines, Safety Testing of Drug Metabolites, in 2008. Metabolite concentrations may accumulate on repeated drug administration and sometimes it may be more appropriate to define the kinetics of a drug via its metabolite.

A similar situation applies to quantification of a drug in urine or faeces. The investigation may be to determine the proportion of drug that is metabolized as part of a mass-balance study or it may be important that the drug is excreted via the urine, for example in the case of diuretics or antimicrobical drugs intended for treating urinary tract infections. On the other hand the excretion rate may be used to define the kinetics of drug and or its metabolite. As far back as 1929 Gold and DeGraff studied the intensity and duration of the effect of digitalis, which to a large extent reflects urinary excretion of digoxin, and demonstrated that elimination results from a fixed proportion, not a fixed amount, of the body content leaving the body in each 24-hour period.

6.2 Metabolite kinetics

It may not be possible to study the kinetics of all the metabolites of a drug. For example, it is unlikely that *all* of the metabolites of any drug will have been identified. Also, when a metabolite is the product of sequential metabolism in an organ such as the liver, the intermediate metabolites may not be released into the bloodstream. Similarly, a metabolite may be formed in the liver and excreted in the bile without entering the general circulation. Thus, we will be considering metabolites that reach the systemic circulation and will assume, in the main, first-order input and output from a single-compartment.

6.2.1 Basic concepts

The time course of a metabolite or metabolites, and hence its or their kinetics, can be influenced by a number of factors and consequently complex relationships are possible. The simplest case would be when all the

Drug Disposition and Pharmacokinetics: From Principles to Applications Stephen H. Curry and Robin Whelpton
 ISBN: 978-0-470-68446-7

administered drug, D, is converted to one metabolite, M, which is then eliminated, either by further metabolism or excretion:

$$\mathrm{D} \xrightarrow{k_{\mathrm{m}}} \mathrm{M} \xrightarrow{k_{\mathrm{m\cdot z}}} \text{elimination}$$

where k_{m} is the rate constant of formation and $k_{\mathrm{m\cdot z}}$ the rate constant of elimination of the metabolite. This situation is analogous to first-order absorption into and elimination from a single compartment model and the equation, which gives the concentration of metabolite, C_{m}, in plasma at any time, t, takes the same form as Equation 4.17:

$$C_{\mathrm{m}} = D\frac{k_{\mathrm{m}}}{V_{\mathrm{m}}(k_{\mathrm{m}}-k_{\mathrm{m\cdot z}}t)}[\exp(-k_{\mathrm{m\cdot z}}t)-\exp(-k_{\mathrm{m}}t)] \tag{6.1}$$

where V_{m} is the volume of distribution of the metabolite. For Equation 6.1 to be valid the dose, D, should be in moles, or corrected for the differences in the relative molecular masses of the drug and metabolite. If the drug is also eliminated via other pathways then D needs to be corrected for the fraction of metabolite formed, f_{m}.

The elimination half-life of a metabolite may be longer or shorter than that of the drug. Because metabolites tend be more polar than the parent drug then the volume of distribution and the degree of reabsorption by the kidney are usually less that those of the parent drug. Consequently, the elimination half-life of the metabolite is shorter. Thus, if the drug and metabolite were injected intravenously, on separate occasions then the amount of metabolite in the body would decline more rapidly [Figure 6.1(a)]. Because metabolites are rarely licensed for use in human beings, metabolite kinetics are usually studied after administration of parent drug. When $k_{\mathrm{m\cdot z}} > k_{\mathrm{m}}$, the rate of formation is rate-limiting and the drug and

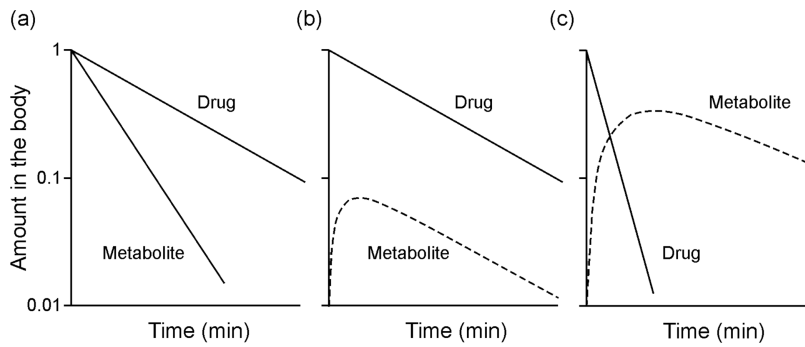

Figure 6.1 (a) Amount of drug and metabolite in the body (as a fraction of dose given) when the half-life of the metabolite is shorter than that of the drug following an i.v. dose of each. (b) Same drug and metabolite as in (a), but when only the parent drug is injected. (c) Situation when the metabolite has a longer half-life than the parent drug.

metabolite concentrations decline in parallel [Figure 6.1(b)]. The term $\exp(-k_{\mathrm{m\cdot z}}t)$ approaches zero faster than $\exp(-k_{\mathrm{m}}t)$ so that at later times the slope of the terminal phase of metabolite curve is $-k_{\mathrm{m}}$, that is the same as that of the parent drug. The situation with regard to the metabolite concentrations is analogous to 'flip-flop' (Section 4.2.4.2) when, without further information, it is not possible to assign the rate constants. When k_{m} is the larger rate constant, $\exp(-k_{\mathrm{m}}t)$ approaches zero more quickly and so the slope of terminal phase for the metabolite is $-k_{\mathrm{m\cdot z}}$ [Figure 6.1(c)].

As already implied, regulations generally prevent human dosing for measurement of the kinetics of drug metabolites except when they are administered as the precursor parent drugs. However, it is possible to learn much from a limited number of examples where a drug and its metabolite(s) are separately approved for medical use. Table 6.1 is a compilation of pharmacokinetic data for ten compounds related in this way. Group I consists of three pairs of drugs, carbamazepine and its epoxide metabolite, codeine and morphine, and *N*-acetyl procainamide and procainamide; in each pair, the half-life of the metabolite administered in its own right is shorter than that of the parent drug. These examples show data of the type in Figure. 6.1(a) after administration of the two drugs separately, but of the type in Figure 6.1(b) after administration of the parent drugs. Note that procainamide and *N*-acetylprocainamide are in fact interconverted. Group II includes three pairs, caffeine and theophylline, amitriptyline and nortriptyline, and imipramine and desipramine; in each pair the half-life of the metabolite is longer than that of the parent drug. These examples show data of the type in Figure 6.1(c) after administration of the parent drugs. The other data in the table is for four benzodiazepines that are related to each other in various ways as precursors and metabolites (Figure 3.7), providing a challenge for the intellectually curious. The half-life relationships in this table show no consistent relationship

Table 6.1 A compilation of pharmacokinetic data for examples of drug pairs used in patients where there is a relation within each pair of precursor and metabolite

Drug example	Protein binding (%)	Half-life (h)	V (l kg^{-1})	CL (ml min^{-1} kg^{-1})	Urinary excretion (%)	Metabolic reaction
Group 1						
Carbamazepine	74	15 (36)[a]	1.4	1.3 (0.36)[a]	<1	
Carbamazepine-10,11-epoxide	50	7.4	1.1	1.7[b]	<1	Epoxide formation
Codeine	7	2.9	2.6	11[b]	0	
Morphine	35	1.9	3.3	24	4–14	*O*-demethylation
N-Acetylprocainamide	10	6	1.4	3.1	81	
Procainamide	16	3	1.9	2.7	67	Hydrolysis
Group II						
Caffeine	36	4.9	0.61	1.4	1.1	
Theophylline	56	9.0	0.5	0.65	18.0	*N*-demethylation
Amitriptyline	94.8	21 (19.5)[c]	15	11.5	<2	
Nortriptyline	92	31 (41.5)[c]	18.4	7.2	2	*N*-demethylation
Imipramine	90.1	12	18	15	<2	
Desipramine	82	22	20	10	2	*N*-demethylation
Benzodiazepines						
1. Diazepam	98.7	43	1.1	0.38	<1	1 to 2, *N*-demethylation
2. Nordazepam	97.5	73	0.78	0.14	<1	1 to 3, hydroxylation
3. Temazepam	97.6	11	0.95	1.0	<1	2 to 4, hydroxylation
4. Oxazepam	98.8	8	0.6	1.05	<1	3 to 4 *N*-demethylation

All data from Goodman and Gilman and so represent interpretations of multiple publications except data in parentheses for amitriptyline.
[a] Data in parentheses from single doses – other data from long-term treatment (carbamazepine is a self-inducer)
[b] Data from CL/F; clearance data for carbamazepine metabolite from renal clearance
[c] Data in parentheses from amitriptyline and nortriptyline measured after amitriptyline doses (Curry *et al*., 1985, 1986, 1987, 1988)

with other pharmacokinetic parameters of the drugs concerned, with the notable exception that *N*-demethylation appears to cause a lengthening of the half-life. A cursory search through the pharmacokinetic literature concerning drugs and their metabolites that are not administered in their own right reveals a preponderance of examples of the Figure 6.1(b) type, suggesting that the case exemplified by carbamazepine and its epoxide is the most common.

The examples of Figure 6.1 consider the *amount* of the substances in the body, and when formation is rate-limiting metabolite is removed almost as soon as it has been formed and so the amount of metabolite at any time is less than that of the drug [Figure 6.1(b)]. However, it is usual to measure the *concentrations* of metabolite, and these will be influenced by their apparent volumes of distribution (Equation 6.1). Increased polarity and, possibly, increased plasma protein binding, particularly of acidic metabolites to albumin, reduces the apparent volume of distribution relative to that of the parent drug. Consequently, the *plasma concentrations* of a metabolite can be much higher than those of the drug, even if the *amounts* in the body are considerably less.

The rate of change of amount of metabolite in the body, dA_m/dt, at any time will be the difference in rates of formation and elimination. The rates are given by the plasma concentration multiplied by clearance (Equation 4.3). Thus:

$$\frac{dA_m}{dt} = C \cdot CL_f - C_m \cdot CL_m \tag{6.2}$$

where CL_f is the clearance associated with the formation of metabolite. Integration of Equation 6.2 gives:

$$\frac{AUC_m}{AUC} = \frac{CL_f}{CL_m} \tag{6.3}$$

6.2.2 Fraction of metabolite formed

The amount of metabolite formed, A_m, can be calculated from the area under the plasma concentration–time curve, AUC_m, provided the clearance, CL_m, is known. This will require intravenous administration of the metabolite. By analogy with Equation 4.13:

$$AUC_m = \frac{A_m}{CL_m} \tag{6.4}$$

so

$$A_m = AUC_m \times CL_m \tag{6.5}$$

and the fraction produced is

$$f_m = \frac{A_m}{D} \tag{6.6}$$

An alternative method when it is not possible to administer metabolite is to use excretion rate data. This approach is only applicable when (i) the rate of formation is rate-limiting, (ii) all the metabolite is excreted via the urine, and (iii) there is no metabolism by the kidney. Under these conditions the rate of metabolite excretion approximately equals the rate of metabolism:

$$\text{Rate of renal excretion of metabolite} \approx C \times CL_f \tag{6.7}$$

Measuring the rate of excretion and the plasma drug concentration allows CL_f to be calculated and substituted into Equation 6.3 to solve for CL_m.

6.2.3 More complex situations

In the majority of cases, the drug will have been given extravascularly, probably orally, and more than one metabolite will be formed. This formation may occur in parallel (Figure 6.2), in sequence (Figure 6.3) or a combination of the two. Furthermore, a proportion of dose may be excreted unchanged.

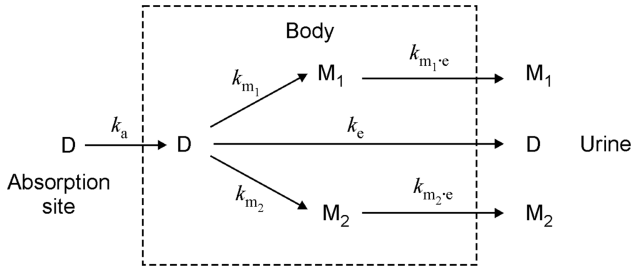

Figure 6.2 A model of metabolism where two metabolites, M_1 and M_2, are produced in parallel. Unchanged drug, D, and the metabolites are excreted into the urine.

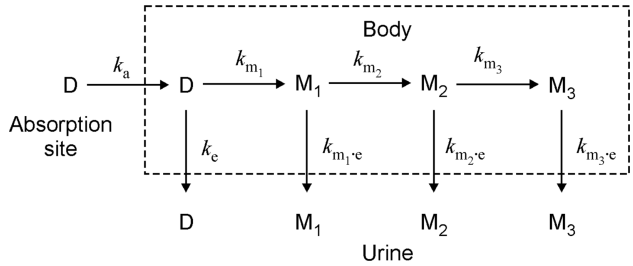

Figure 6.3 A model of excretion where the metabolites, M_1 M_2 and M_3 are produced sequentially. Unchanged drug, D, and metabolites are excreted into urine.

In the case of a single metabolite that is excreted into the urine, the equation relating the amount of metabolite in the body after an i.v. bolus injection of D is:

$$A_m = D\frac{k_m}{(k_{m\cdot e}-\lambda)}[\exp(-\lambda t)-\exp(-k_{m\cdot e}t)] \tag{6.8}$$

where $k_{m\cdot e}$ is the rate constant for urinary excretion of metabolite and the elimination rate constant of the drug is $\lambda = k_m + k_e$. The equation for the amount of metabolite excreted into the urine is:

$$A_{m,\,urine} = D\frac{k_m}{\lambda}\left\{1-\frac{1}{(k_{m\cdot e}-\lambda)}[k_{m\cdot e}\exp(-\lambda t)-\lambda\exp(-k_{m\cdot e}t)]\right\} \tag{6.9}$$

In the case depicted in Figure 6.3 any of the steps may be the rate-limiting one, and so the plasma concentrations of any metabolites formed after the rate-limiting step will decline in parallel. In either case, if the rate of absorption is the slowest step then drug and all the metabolites formed from it will decline with a half-life equivalent to that of absorption.

Complex situations arise when a metabolite is further metabolized by more than one route. This is the case with 4′-hydroxypropranolol. The formation of the 4′-hydroxy metabolite of propranolol is rate-limited,

and so the propranolol and metabolite concentrations fall in parallel (as illustrated later in Figure 6.6). The major routes of metabolism of 4′-hydroxypropranolol are sulfation or glucuronidation and, at first sight, the half-lives of the conjugates appear to be greater than that of 4′-hydroxypropranolol [Figure 6.4(a)], even though these metabolites would be expected to be more readily excreted. In fact the longer elimination half-lives arise because the kinetics are formation rate-limited and the decline in plasma concentrations are controlled by the relatively slow rate of formation. In this situation the half-life of 4′-hydroxypropranolol is shorter than apparent half-lives of the individual conjugates because it is being metabolized by (at least) two routes. That the apparent elimination half-life of sulfate was formation-rate limited was confirmed by administering the conjugate on a separate occasion, when the half-life was 82 ± 12 min rather than 156 ± 21 min when it was a metabolite of 4′-hydroxypropranolol.

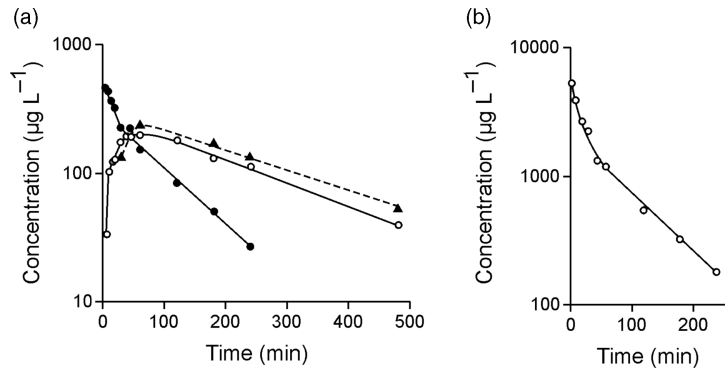

Figure 6.4 Plasma concentrations of 4′-hydroxypropranolol (•) and its sulfate (○) and glucuronide (▲) conjugates (a) after i.v. injection of 4′-hydroxypropranolol, 2 mg kg^{-1} in dogs. (b) Plasma concentrations of 4′-hydroxypropranolol sulfate after i.v. injection of 2 mg kg^{-1} in dogs (adapted from Christ *et al.*, 1990).

6.2.4 Active metabolites

The significance of an active metabolite will depend on whether the elimination kinetics of the metabolite are formation dependent or elimination dependent. In the former case the half-life of the metabolite will be the same as that of the parent drug and so it will accumulate at the same rate as does the parent compound. Therefore, dosing can be based upon the disposition parameters for the drug and it is not necessary to be concerned with the kinetic parameters of the metabolite. This even applies to prodrugs where the metabolite is the active species, although in practice a prodrug is likely to have a very short elimination half-life and the rate of formation of the metabolite will not be rate limiting. Under these circumstances the metabolite will be monitored and the dosing will be based on the kinetics of the metabolite.

When the kinetics are elimination dependent, the half-life of the metabolite is greater than the drug and so the metabolite continues to accumulate after the drug has reached steady-state conditions, for example during a continuous infusion or on multiple dosing. Because the metabolite takes longer to reach steady-state, dosing should be determined by the disposition characteristics of the metabolite. The average concentration of metabolite at steady-state can be calculated from the AUC_m after a single i.v. dose:

$$C_{av}^{ss} = \frac{AUC}{\tau} \tag{6.10}$$

See also Equation 4.38. Furthermore, the frequency of dosing should be based on the half-life of the metabolite, i.e. it is not necessary to give the drug as frequently as the half-life of the drug might suggest.

The *N*-desmethyl metabolites of several centrally acting drugs, including imipramine and amitriptyline, show pharmacological activity similar to that of the parent drug and tend to accumulate to higher concentrations than the parent drug on multiple dosing. Nordazepam is a metabolite of several 7-chlorobenzodiazepine drugs and, because of its long elimination half-life accumulates to concentrations greater than those of the parent drug. In human beings steady-state concentrations of nordazepam are approximately twice those of diazepam after repeated administration of the latter [Figure 6.5(a)].

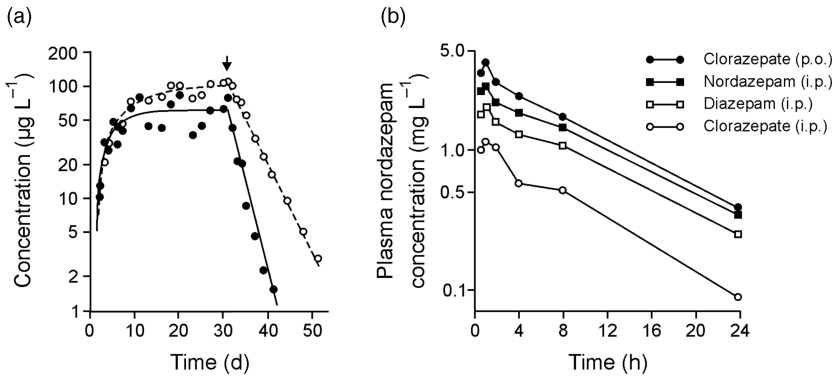

Figure 6.5 (a) Plasma diazepam (•) and nordazepam (o) concentrations in a healthy female volunteer after 2 mg diazepam at night for 30 days (redrawn from Abernethy *et al.*, 1983). (b) Plasma nordazepam concentrations after dosing with clorazepate (4.5 mg kg^{-1}), diazepam and nordazepam (3.0 mg kg^{-1}) (from the data of Curry *et al.*, 1977).

Because the kinetics of nordazepam are not formation dependent then the plasma half-life should be independent of the drug that is administered. This is illustrated in Figure 6.5(b) where diazepam or clorazepate, a prodrug which decomposes to nordazepam in gastric acid, was administered. As predicted the half-life of the metabolite was the same as when nordazepam was injected. The amount of nordazepam produced following i.p. injection of clorazepate was markedly reduced – illustrating the role of gastric acid in the formation of the active moiety [Figure 6.5(b)].

6.2.5 Effect of presystemic metabolism

When drugs are taken orally and undergo extensive presystemic metabolism, both drug and metabolite appear in the systemic circulation together. This is like taking a mixture of drug and metabolite. For a metabolite that displays formation rate-limited disposition it would be expected that drug and metabolite peak plasma concentrations would occur at the same time and then decline in parallel (Figure 6.6).

However, the initial concentrations of metabolite in the plasma are not dependent on rate-limited formation from the parent drug and decline according to the disposition kinetics of the metabolite, that is, as if the metabolite had been administered rather than the drug. This results in a bi-exponential decline in metabolite concentrations after oral administration of parent drug (Figure 6.6). It is important not to confuse this bi-exponential decay with that seen for two-compartment models.

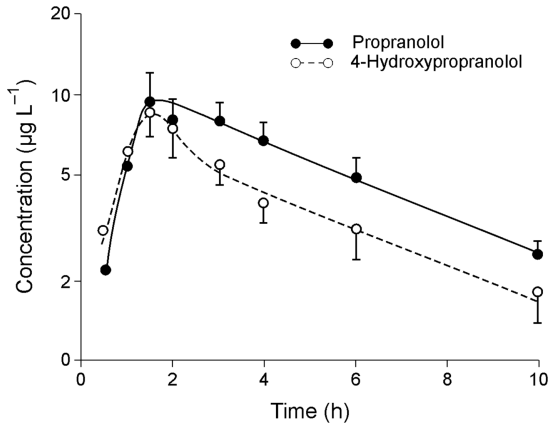

Figure 6.6 Mean plasma concentrations of propranolol and its 4′-hydroxymetabolite after oral administration of propranolol (20 mg) to six normal volunteers. Error bars represent mean ± SEM. (Redrawn from Walle *et al.*, 1980.)

When first-pass metabolism occurs primarily in the liver then the AUC_m values after oral and intravenous doses should be similar, provided, of course, that all the dose of drug is absorbed. This is because the drug can enter the liver whether it is given orally or by injection. Consequently for a drug with low oral bioavailability, the areas under the metabolite plasma concentration–time curves can be used to differentiate poor absorption from extensive hepatic first-pass metabolism. If the AUC_m is higher after an oral dose than when the drug is injected, then this is indicative that presystemic metabolism is occurring in the GI tract.

6.2.6 Interconversion of drug and metabolite

Some metabolites may be converted back to parent drug as depicted below:

$$\begin{array}{ccc} \text{Drug} & \rightleftharpoons & \text{Metabolite} \\ \downarrow & & \downarrow \\ \text{Elimination} & & \text{Elimination} \end{array}$$

The drug and metabolite may also be eliminated via other routes, either further metabolism or excretion. This model is analogous to a two-compartment model, with loss from both the central and peripheral compartments. Initially drug concentrations fall rapidly but as drug and metabolite concentrations equilibrate interconversion has a major influence on the half-life of the drug and metabolite. Several drugs exhibit this phenomenon including: cortisol–cortisone, haloperidol–reduced haloperidol, prednisone–prednisolone, and vitamin K–vitamin K epoxide. The effect of interconversion has been nicely demonstrated for predisone and prenisolone (Figure 6.7). After administration of prednisone, the concentrations of the active metabolite, prednisolone, rose to over 10 times those of prednisone. When prednisolone hemisuccinate was given intravenously the prednisolone concentrations fell rapidly until the prednisolone: prednisone ratio equilibrated at the same value as that after administration of prednisone, demonstrating that interconversion produces the same drug to metabolite ratio irrespective of which drug is given. Prednisolone hemisuccinate is a prodrug ester of prednisolone which is very rapidly hydrolysed to prednisolone.

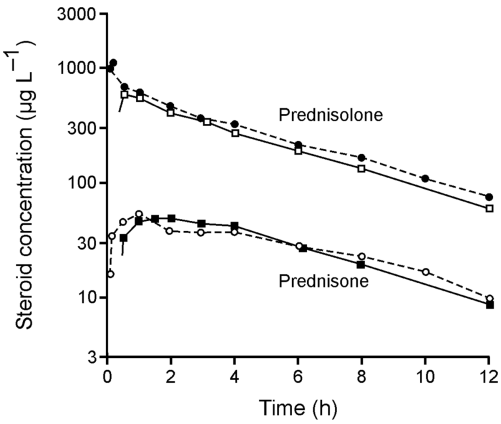

Figure 6.7 Plasma concentrations of prednisone and prednisolone after a single oral dose of prednisone (solid lines) or an i.v. dose of prednisolone hemisuccinate ester to a healthy male volunteer (adapted from Rose *et al.,* 1980).

In the case of sulindac, the sulfide, which is oxidized back to the parent drug, is active whereas the sulfone metabolite is not interconverted and is inactive (Figure 6.8). Thus, sulindac is a prodrug, and it has been suggested that this is why it is less prone to cause gastrointestinal upsets when compared with some other non-steroidal anti-inflammatory drugs as the active form is not produced until after absorption.

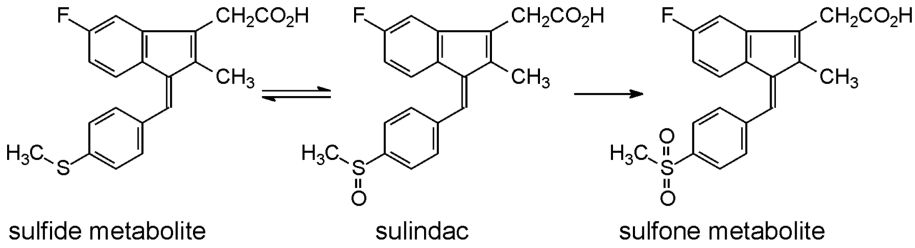

Figure 6.8 Sulindac (a sulfoxide) is reversibly reduced to pharmacologically active sulfide or oxidized to sulfone metabolite.

6.3 Renal excretion

The factors contributing to urinary excretion of a compound are:

- Glomerular filtration
- Passive reabsorption from renal tubular fluid
- Pctive secretion into renal tubular fluid.

These were discussed in Section 3.3.1.

6.3.1 Kinetics of urinary excretion

Glomerular filtration and diffusion across the renal tubular epithelium are generally first-order processes so that the rate of transfer of drug is related to the amount of drug in plasma. The excretion of a drug in urine is

complicated by further factors including:

- The concentration of drug in renal tubular fluid is influenced by changes in urine volume so there is a tendency for the concentration to increase as water is reabsorbed by the kidney.
- Changes in urinary pH can influence the rates at which weak electrolytes are excreted.

Therefore it is usual to relate the *rate* of renal elimination to the concentration of drug in plasma. The differential equation for the rate of appearance of drug in urine is:

$$\frac{\mathrm{d}Ae}{\mathrm{d}t} = k_e A \tag{6.11}$$

where Ae is the amount of drug excreted in urine at time t and k_e is the first-order rate constant for urinary elimination. A is given by:

$$A = D\exp(-\lambda t) \tag{6.12}$$

so

$$\frac{\mathrm{d}Ae}{\mathrm{d}t} = k_e D\exp(-\lambda t) \tag{6.13}$$

Integrating Equation 6.13 gives:

$$Ae = \frac{k_e}{\lambda} D[1-\exp(-\lambda t)] \tag{6.14}$$

The total amount of drug excreted in the urine, $Ae(\infty)$ is

$$Ae(\infty) = \frac{k_e}{\lambda} D \tag{6.15}$$

indicating that the fraction of an intravenous dose that is eventually excreted into the urine is given by the ratio of the rate constants for urinary excretion and elimination.

A semilogarithmic plot of *excretion rate* versus time should give a straight line of slope $-\lambda$ (Equation 6.13). In practice the excretion rate is calculated from urine samples collected at discrete intervals and the data are either plotted as a histogram or the mid-points of the collection period are used. This approach assumes that there are no changes in the rate of renal excretion as a result of fluctuations in urinary pH, urine volume or unknown factors. To reduce the effects of fluctuations seen in excretion rate plots, an alternative approach is the 'sigma-minus' method. Urine is collected for sufficiently long to allow estimation of $Ae(\infty)$ – this should be for up to about seven elimination half-lives. Substituting Equation 6.15 into Equation 6.14 and rearranging gives:

$$Ae(\infty) - Ae = Ae(\infty)\exp(-\lambda t) \tag{6.16}$$

A semilogarithmic plot of percent of drug remaining to be excreted against time is a straight line of slope $-\lambda$.

Similar approaches can be used to derive equations for urinary excretion following first-order absorption into a single-compartment model, elimination from a two-compartment model and non-linear kinetics.

6.3.1.1 Renal clearance

The rate of elimination of a drug is the systemic clearance multiplied by the plasma concentration (Equation 4.3) The urinary excretion rate is the renal clearance, CL_R, multiplied by the plasma concentration, so:

$$CL_R = \frac{dAe/dt}{C} = \frac{k_e A}{C} \tag{6.17}$$

Note that Equation 6.17 is consistent with the physiologists' definition of renal clearance (Equation 3.6). Because A/C is the apparent volume of distribution, Equation 6.17 can be rewritten:

$$CL_R = k_e V \tag{6.18}$$

Equation 6.18 gives a route to determining k_e, provided that the apparent volume of distribution of the drug is known (from an intravenous injection) and the renal clearance is measured using Equation 3.6.

6.3.1.2 Effect of urine flow rate

The effect of urine flow rate will depend on whether the plasma and urine concentrations have equilibrated. At equilibrium, U/P (Equation 3.6) will be constant and renal clearance will be directly proportional to urine flow rate. Furthermore, for a neutral molecule that binds to plasma protein the urine concentration and the unbound concentration of drug in plasma will be equal at equilibrium so renal clearance will be:

$$CL_R = f_u \times \text{urine flow rate} \tag{6.19}$$

where f_u is the fraction of unbound drug in plasma. An alternative way of visualizing the effect of flow rate is that if the urine and plasma concentrations have more or less equilibrated then by whatever proportion the urine flow rate is increased then the *amount* of drug in urine must increase by the same proportion to maintain the required urine concentration. Ethanol, which is not bound to plasma proteins, does not ionize and usually equilibrates rapidly shows a nearly linear relationship between renal clearance and urine flow rate with a slope close to 1 [Figure 6.9(a)]. Correlations between urine flow and clearance have been shown for other drugs, including phenobarbital, sulfafurazole and glutethimide [Figure 6.9(b)]. For glutethimide, the clearance is less than the urine flow rate, which in part can be explained by the fact that drug is approximately 50% bound to plasma proteins. Urine flow will not have much influence on the clearance of drugs for which there is little renal tubular reabsorption.

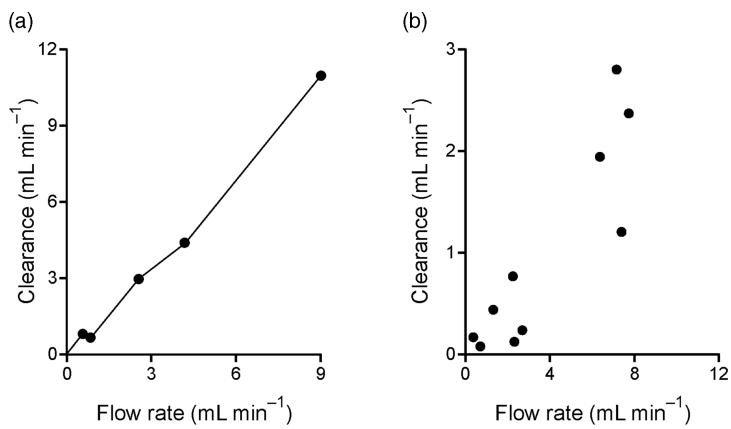

Figure 6.9 Renal clearance as a function of urine flow rate: (a) ethanol, data are five independent estimates in one subject and (b) glutethimide, data are 10 independent estimates.

Despite the increased clearance of some drugs with increased urine flow, forced acidic or alkaline diuresis is no longer employed for treating drug overdose because the changed fluid balance is considered potentially dangerous. Sodium bicarbonate may be used to increase the renal clearance of salicylate and chlorophenoxyacetic acid herbicides, such as 2,4-dichlorophenoxyacetic acid (2,4-D) and 2,3,5-trichlorphenoxyacetic acid (2,3,5-T), but an additional diuretic is not used.

6.3.2 Specific drug examples

6.3.2.1 Amphetamine

The effect of urine volume and pH on the excretion rate of amphetamine is shown in Figure 6.10. There is a clear relationship between the excretion rate and urine pH as would be expected for this weak base ($pK_a \sim 9.8$). There is also an indication that the excretion rate increases with increasing urine volume. Obviously it is not possible to derive pharmacokinetic parameters under the conditions of Figure 6.10, but values have been obtained when the urine pH was adjusted to, and maintained at, ~pH 5 with the administration of ammonium chloride. Under these conditions the renal excretion of amphetamine is markedly increased (c.f. Figure 3.18) which must have an effect on any half-life value calculated.

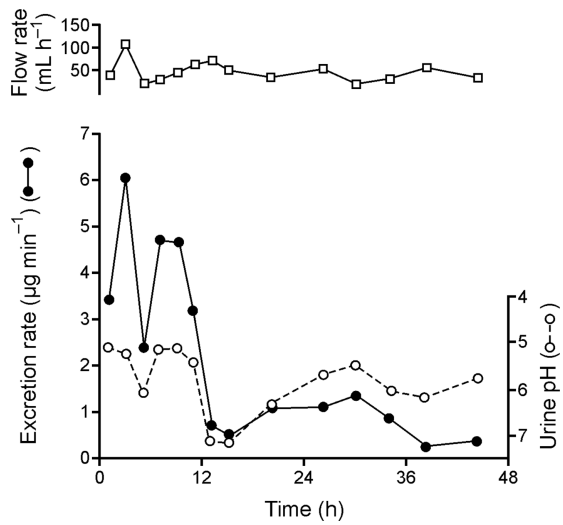

Figure 6.10 Effect of urine pH and volume on the urinary excretion of amphetamine in a single human subject, after oral administration of 10 mg amphetamine sulfate. (Redrawn from Beckett and Rowland 1964.)

6.3.2.2 Ethanol

Ethanol distributes freely with total body water. In spite of wide variations in the volume of urine produced, the concentration of ethanol in urine is closely related to its concentration in blood (Figure 6.11). In the case of ethanol, diffusion of the drug between urine and blood apparently occurs up to a time not long before the urine is removed from the body.

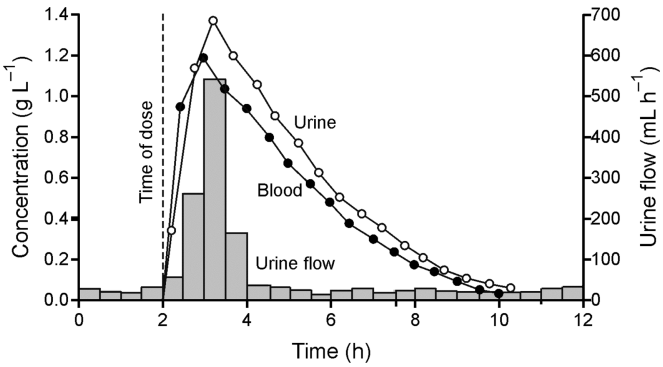

Figure 6.11 Concentrations of ethanol in whole blood (•) and urine (○) after an oral dose of 64 g of ethanol with 116 mL of water. Note that the urine concentrations are plotted at the midpoint of the collection interval (after Haggard *et al.*, 1941).

The near constant ratio of blood to urine concentrations allows urine to be used as an alternative to blood for the purposes of 'drink-driving' laws – 1.07 g L^{-1} in urine being equivalent to 0.8 g L^{-1} (0.08%) in blood.

6.3.2.3 Fluphenazine

Fluphenazine is usually administered as an i.m. depot injection of its decanoate ester, a prodrug, which is hydrolysed to fluphenazine and released into the plasma. Before the advent of sufficiently sensitive assays, fluphenazine kinetics could only be studied by administration of radiolabelled drug or from urinary excretion studies. In man, fluphenazine is present in urine as fluphenazine plus conjugates that can be released by hydrolysis with β-glucuronidase. Using ^{14}C-labelled drug the relationship between the plasma concentration and urinary excretion rate of fluphenazine plus conjugates was demonstrated [Figure 6.12(a)]. Having

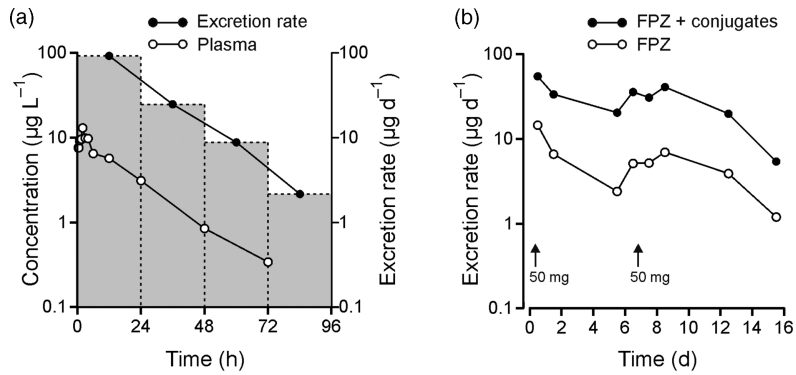

Figure 6.12 (a) Plasma concentrations and urinary excretion rate of fluphenazine after an intramuscular injection of 25 mg. (b) Urinary excretion rate of fluphenazine and conjugated fluphenazine in a patient receiving 50 mg fluphenazine decanoate (i.m.) weekly (after Whelpton and Curry, 1976).

established this relationship, the kinetics of fluphenazine after intramuscular injection of the decanoate ester (50 mg weekly) to a psychiatric inpatient were investigated by following the renal excretion of either the drug or drug plus conjugated metabolites [Figure 6.12(b)]. The excretion rates of conjugated metabolites parallel those of fluphenazine as would be expected for a metabolite whose disposition kinetics are formation-limited. This is an example where the parent drug was a prodrug and the kinetics were studied by monitoring the urinary excretion of a metabolite of the pharmacologically active compound, fluphenazine.

6.4 Excretion in faeces

Drugs and their metabolites that are excreted via the bile are either reabsorbed, or remain in the GI tract to be removed in the faeces, as explained in Section 3.3.2. Although it is rarely done, it is possible to determine drug kinetics from faecal excretion data, as exemplified below for the photodynamic agent, temoporfin. The same arguments as those made for renal excretion apply. Temoporfin was particularly suitable because (i) it is administered by intravenous injection so any drug or metabolite in the faeces is there because it has been excreted, (ii) over 99% is eliminated in faeces and (iii) it has a long elimination half-life. A study with non-radiolabelled drug indicated that the terminal half-life in BALB/c mice was at least 13.9 h but, as it was possible to measure the drug in blood for only 48 h, this was considered to be an underestimate (Whelpton *et al*., 1995). The slow decline in temoporfin concentrations in some tissues, notably lung and kidney, which were monitored for 96 hours confirmed this view. When ^{14}C-temoporfin became available the study was repeated and the drug monitored for up to 35 days. Faecal excretion rates are shown in Figure 6.13. The decay was bi-exponential

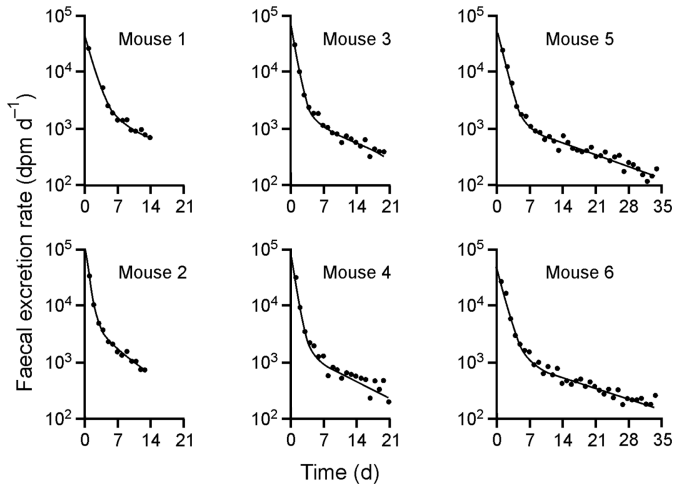

Figure 6.13 Faecal excretion of ^{14}C-label following temoporfin administration to BALB/c mice; solid lines are the least squares fit of the data to a two-compartment model (from Whelpton *et al.*, 1996).

A putative metabolite was detected in liver and faeces but not in blood nor any other tissue. This is in keeping with a metabolite that is produced in, and excreted by, the liver, probably via bile. The metabolite concentrations declined in parallel with those of temoporfin indicating that its disposition was formation

rate-limited. Thus, it was possible to define the disposition of temoporfin by monitoring the rates of faecal excretion for up to 7 weeks.

The data of Figure 6.13 illustrate another important point – it is necessary to ensure that the data are collected for sufficient time to derive a reliable estimate of the half-life of the terminal phase. Failure to do so will result in an underestimate (Table 6.2).

Table 6.2 Elimination half-lives derived from faecal excretion data of Figure 6.13

Mouse	Duration 0–14 days[a]		Duration 0–21 days		Duration 0–28 days	
	$t_{1/2}$ (λ_1) (h)	$t_{1/2}$ (λ_2) (days)	$t_{1/2}$ (λ_1) (h)	$t_{1/2}$ (λ_2) (days)	$t_{1/2}$ (λ_1) (h)	$t_{1/2}$ (λ_2) (days)
1	22.7	9.0				
2	13.0	5.0				
3	15.4	8.7	14.6	7.3		
4	14.9	6.2	15.4	7.5		
5	18.0	6.5	19.9	10.5	20.2	11.0
6	18.2	5.8	21.2	10.2	21.1	10.0
Mean	17.0	6.9	17.8	8.9	20.7	10.5

[a] Time over which kinetic parameters were calculated.

References and further reading

Abernethy DR, Greenblatt DJ, Divoll M, Shader RI. Prolonged accumulation of diazepam in obesity. *J Clin Pharmacol* 1983; 23: 369–76.

Beckett AH, Rowland M. Rhythmic urinary excretion of amphetamine in man. *Nature* 1964; 204: 1203–4.

Christ DD, Walle UK, Oatis JE, Jr., Walle T. Pharmacokinetics and metabolism of the pharmacologically active 4′-hydroxylated metabolite of propranolol in the dog. *Drug Metab Dispos* 1990; 18: 1–4.

Curry SH, Whelpton R, Nicholson AN, Wright CM. Behavioural and pharmacokinetic studies in the monkey (*Macaca mulatta*) with diazepam, nordiazepam and related 1,4-benzodiazepines. *Br J Pharmacol* 1977; 61: 325–30.

Curry SH, DeVane CL, Wolfe MM. Cimetidine interaction with amitriptyline. *Eur J Clin Pharmacol* 1985; 29: 429–433.

Curry SH, DeVane CL, Wolfe MM. Pharmacology of combined antidepressant/H_2-blocking drug therapy. *Psychopharmacol Bull* 1986; 22: 220–222.

Curry SH, DeVane CL, Wolfe MM. Lack of interaction of ranitidine with amitriptyline. *Eur J Clin Pharmacol* 1987; 32: 317–320.

Curry SH, DeVane CL, Wolfe MM. Hypotension and bradycardia induced by amitriptyline in healthy volunteers. *Human Psychopharmacology* 1988; 3: 47–52.

Duggan DE. Sulindac: therapeutic implications of the prodrug/pharmacophore equilibrium. *Drug Metab Rev* 1981; 12: 325–37.

http://www.fda.gov/downloads/Drugs/GuidanceComplianceRegulatoryInformation/Guidances/ucm079266.pdf (accessed 28th July 2009).

Gold H, Degraff AC. Studies on digitalis in abulatory cardic patients: II. The elimination of digitalis in man. *J Clin Invest* 1929; 6: 613–26.

Haggard HW, Greenberg LA, Carroll RP. Studies in the absorption, distribution and elimination of alcohol: VIII. The diruesis from alcohol and its influence on the elimination of alcohol in the urine. *J Pharmacol Exp Ther* 1941; 71: 349–357.

Rose JQ, Yurchak AM, Jusko WJ, Powell D. Bioavailability and disposition of prednisolone tablets. *Biopharm Drug Dispos* 1980; 1: 247–58.

Walle T, Conradi EC, Walle UK, Fagan TC, Gaffney TE. 4-Hydroxypropranolol and its glucuronide after single and long-term doses of propranolol. *Clin Pharmacol Ther* 1980; 27: 22–31.

Whelpton R, Curry SH. Methods for study of fluphenazine kinetics in man. *J Pharm Pharmacol* 1976; 28: 869–73.
Whelpton R, Michael-Titus AT, Basra SS, Grahn M. Distribution of temoporfin, a new photosensitizer for the photodynamic therapy of cancer, in a murine tumor model. *Photochem Photobiol* 1995; 61: 397–401.
Whelpton R, Michael-Titus AT, Jamdar RP, Abdillahi K, Grahn MF. Distribution and excretion of radiolabeled temoporfin in a murine tumor model. *Photochem Photobiol* 1996; 63: 885–91.